Supporting information

Metal Free Azophenine based Electrocatalyst: A Promising Approach Towards Sustainable Alkaline Hydrogen Evolution

Sandip Kumar Tudu,[a,b] Debojyoti Kundu,[a,b] Sanjukta Zamindar,[a,b] Riyanka Das,[c] Sunanda Maji,[a,b] Priyabrata Banerjee*[a,b]

[a] *Electric Mobility and Tribology Research Group, CSIR – Central Mechanical Engineering Research Institute (CMERI), Mahatma Gandhi Avenue, Durgapur, 713209, West Bengal, India*

[b] *Academy of Scientific and Innovative Research (AcSIR), Ghaziabad, 201002, India*

[c] *International Institute for Sustainability with Knotted Chiral Meta Matter (WPI-SKCM^2), 2-313 Kagamiyama, Higashi-Hiroshima City, Hiroshima, Japan 739-0046.*

**Corresponding author:*

Priyabrata Banerjee, E-mail address: pbanerjee.cmeri@csir.res.in

General information

Materials

All chemicals were purchased commercially and used without further purification Ferric Chloride hexahydrate ($FeCl_3.6H_2O$), ortho Anisidine, potassium hydroxide (KOH), Platinum on Carbon (10 wt. %), 2-Propanol, methanol, absolute ethanol and acetone were purchased from Sigma-Aldrich, dichloromethane (DCM), hexane were purchased from Merck India Pvt. Ltd. Deionized water was used throughout all experiments.

Instrumentation

FT-IR analysis: FT-IR spectroscopic data were recorded in solid state using KBr pellets on PerkinElmer Spectrum 100 FT-IR spectrometer in the region of 4000-400 cm^{-1}.

^{1}H NMR Analysis: The ^{1}H NMR spectra recorded by ASCEND 400 modelled 400 MHz NMR spectrophotometer (Bruker, USA). The NMR spectra of all the materials were obtained by using DMSO-d_6 solvent.

Powder X-ray diffraction (PXRD) data analysis: Crystallinity and phase purity were analysed by PXRD data. By using a mortar and pestle, 20 mg of the sample was ground into a fine powder. Cu Kα X-ray radiation (λ = 1.5418 Å) was used in a BRUKER D8 Discover diffractometer to obtain the sample's PXRD data at room temperature. Data was collected at a scan rate of 1°/min using a working voltage and current of 40 kV and 20 mA, respectively.

FE-SEM analysis: Surface morphology of synthesised material was analysed by FESEM, Zeiss Sigma microscope, Oxford Instruments, Germany.

HR-TEM analysis: A JEM 2100 (JEOL, Japan) high-resolution transmission electron microscope was used for the microscopic analysis.

X-ray photoelectron spectroscopy: The surface chemical composition of the as synthesised material was further analysed by XPS using PHI 5000 Versa Prode III system with a monochromatic Al Kα (1486.6 eV) X-ray radiation operated at working voltage 15 kV and 20 mA current. A pallet of the compound was used for the measurement after sputtering of 30 sec. The binding energies are calibrated vs. carbon (C1s = 284.6 eV). XPS spectra were deconvoluted by using Origin software.

Inductively Coupled Plasma Mass Spectrometry (ICP-MS): The trace levels of iron species were quantified using inductively coupled plasma mass spectrometry (ICP-MS) on a Thermo Fisher Scientific ICAPRQ instrument. **ME:** Multi Element standards directly purchased from sigma that includes Al, Sb, Ba, Pb, B, Ca, Cd, Cr, Co, Fe, K, Cu, Li, Mg, Mn, Mo, Na, Ni, P, Si, Ti, V, and Zn in 5% nitric acid and ≤0.1 % hydrofluoric acid. **Mix:** Mix Elements prepared using individual standards of Hg + Au + As in 5% nitric acid and ≤0.1 % hydrofluoric acid. **ME + Mix** represents the standard, included all the 25 elements of both sets.

Synthesis procedure

At first the mixture of (950 mg) o-Anisidine and (160 mg) $FeCl_3.6H_2O$ was taken in a culture vial then it was allowed to stand at 90°C for 3hr in presence of air, after that the mixture was extracted in a beaker with Dichloromethane (DCM) and allowed to stand at room temperature for solvent reduction. For separation, Colum chromatography was performed with the help of 1:1 hexane-DCM mixture. A bright red coloured crystalline product was collected.

Electrochemical measurements

All electrochemical assessments were conducted at room temperature by using CHI660B electrochemical workstation. Three-electrode configuration was employed using Pt wire as a counter electrode, Ag/AgCl as a reference electrode and the sample was taken as a working electrode, the working electrode was prepared by using spin-coating on properly edged Ni foam of 1x0.5 cm^2 area. 1M KOH was taken as an electrolyte for further electrochemical studies. Pt/C (10 wt.%) was also taken in the same manner for further comparison. Therefore, the electrochemical studies were assessed by using linear sweep voltammetry (LSV), by scanning the potential range from 0 to -2 V for HER at a scan rate of 10 mV cm^{-1} with respected to the Ag/AgCl as a reference electrode. All potential calculations were converted to Reversible Hydrogen Electrode (RHE) scale using Eq. 1.

$$\boldsymbol{E_{RHE} = E_{appl} + E_{Ag/AgCl} + 0.059 \times pH} \text{ ..... Eq. 1.}$$

Where, E_{appl} is the applied potential of the RHE, the potential of the Ag/AgCl (saturated KCl) reference electrode ($E_{Ag/AgCl}$ = 0.198 V vs RHE, T = 25 °C), and the pH of the electrolyte solution (1M KOH pH~13.9). The impedance was assessed in 1M KOH solution in the range of 10 kHz to 1 Hz for the catalytic behaviour of the material electrode and the electrolyte solution. Double layer capacitance is another parameter for forecasting its catalytic activity by calculating its ECSA. Electrochemical Surface area (ECSA) was calculated by using the Eq. 2.

$$\boldsymbol{ECSA = C_{dl}/C_s} \text{ ..... Eq. 2.}$$

The working electrode was prepared as follows: 4mg of sample was taken in a 400µl of solution, contained 200 µl of 2-propanol and 200 µl of deionised water. In addition, 1mg of PVDF was added into the solution as binder. After that it was allowed to stand at ultrasonication for maintaining the homogeneity. In order to develop the working electrode, 200 µl of prepared solution was drop-casted on a Nikel foam then left to evaporate the solvent.

Computational methods

Density functional Theory (DFT) of the CN-1 was performed by using Dmol3 module in material studio to evaluate the frontier molecular orbitals (FMO). The generalized gradient approximation (GGA) with Perdew–Burke–Ernzerhof (PBE) exchange-corelation function was employed. Based on PXRD data of CN-1, 1x1 supercell was constructed with the facet (010). The surface model (010) was contained of 60 atoms. Moreover, moderate level of calculations was applied using self-consisted field (SCF) convergence creation of 10^{-5} and 100 SCF repetition cycles in combination with DNP basis set. COSMO was chosen as an aqueous solvent during the simulation with the dielectric constant 78.54.

In order to evolute the theoretical prediction of the activity regarding HER on the solid electrode surface free energy calculation plays a vital role. Gibbs free energy of the hydrogen adsorption is derived from the equation mentioned below (Eq. 3).[1]

$$\Delta G_{H^*} = \Delta E_{H^*} + \Delta E_{ZPE} - T\Delta S_H \quad \text{..... Eq. 3.}$$

Where (ΔG_{H^*}) is Gibbs free energy of the adsorbed hydrogen, ($\Delta E_{ZPE)}$ is the zero-point energy, (ΔS_H) is the entropy of adsorption at temperature T.

ΔE_{H^*} was calculated by taking the separated H_2 as a reference state (Eq. 4)

$$\Delta E_{H^*} = E_{(Surface + H^*)} - E_{(Surface)} - \tfrac{1}{2}H_2 \quad \text{.....} \quad \text{Eq. 4.}$$

ΔE_{ZPE} for isolated H_2 or adsorbed H* can be obtained by the (Eq. 5).

$$\Delta E_{ZPE} = \tfrac{1}{2} \sum h\upsilon_i \quad \text{..... Eq. 5.}$$

Where υ_i is the computed vibrational frequencies.

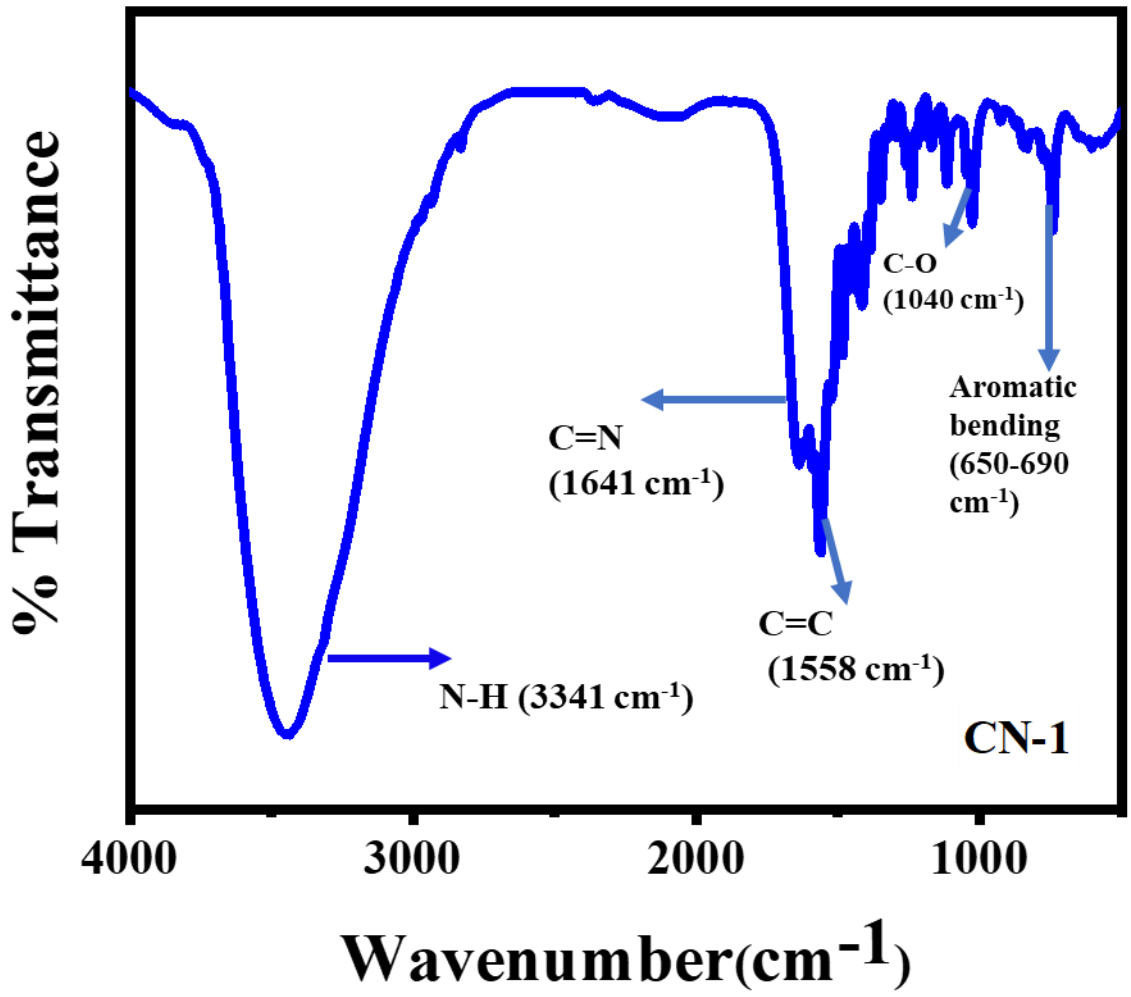

Fig. S1: FT-IR spectra of **CN-1.**

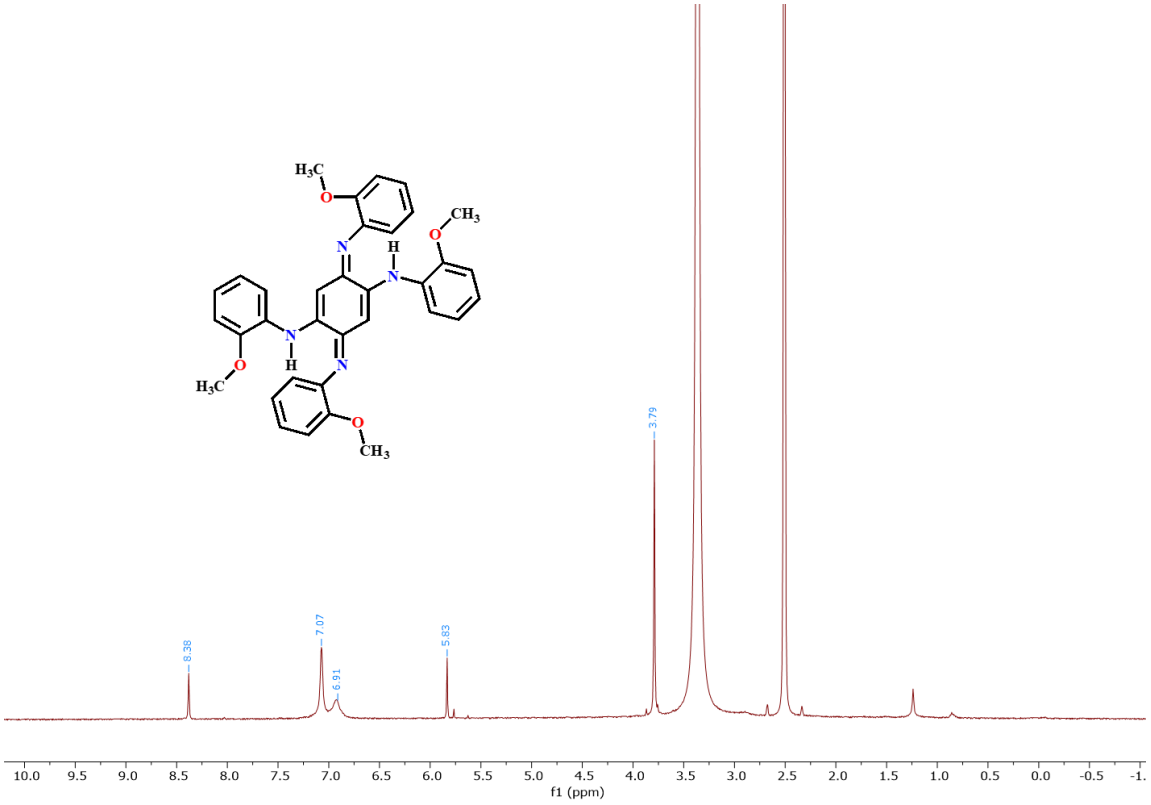

Fig. S2. ^{1}H NMR spectrum of **CN-1** in DMSO-d_6 (400Hz)

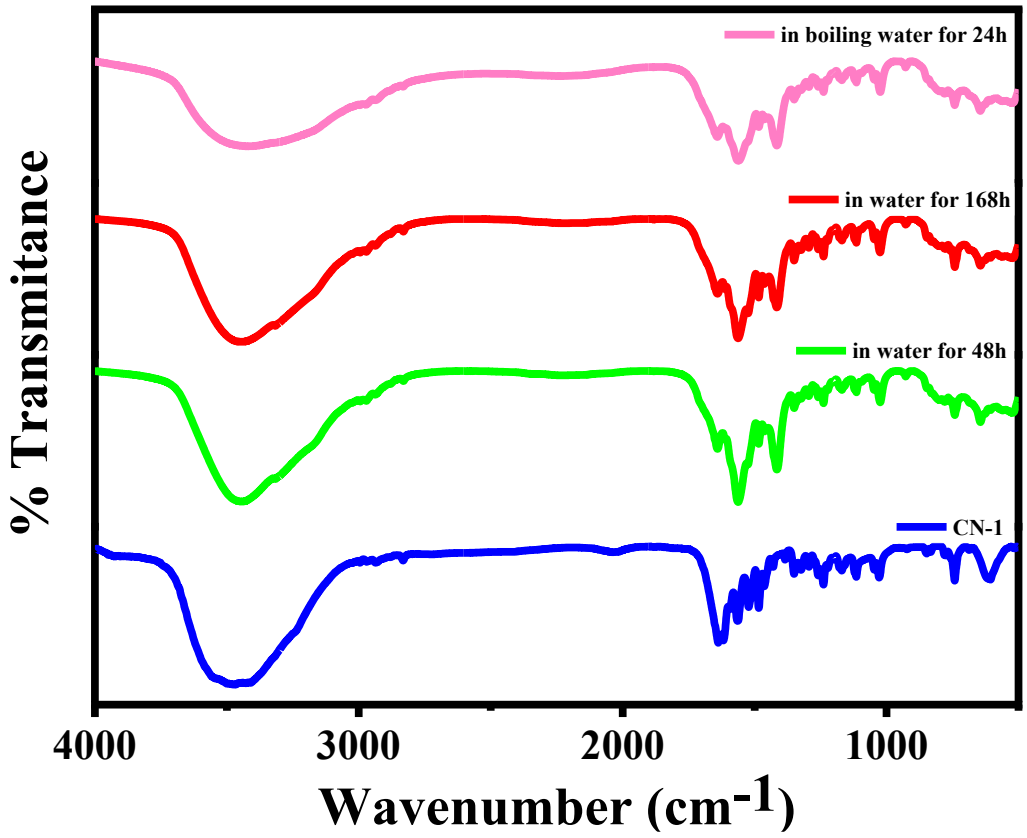

Fig. S3: FT-IR spectra for the Hydrolytic stability of **CN-1.**

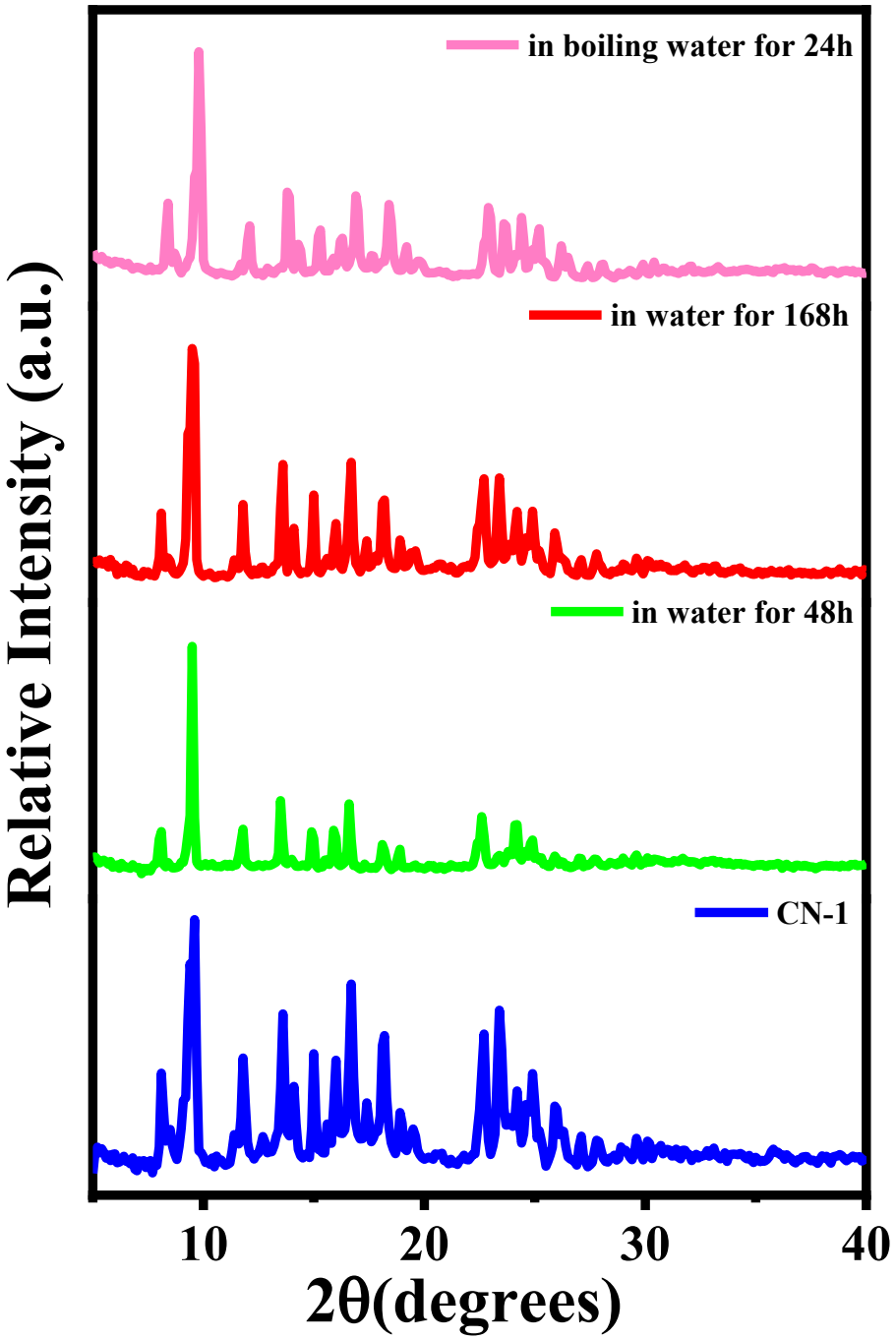

Fig. S4. PXRD patterns for the Hydrolytic stability of **CN-1.**

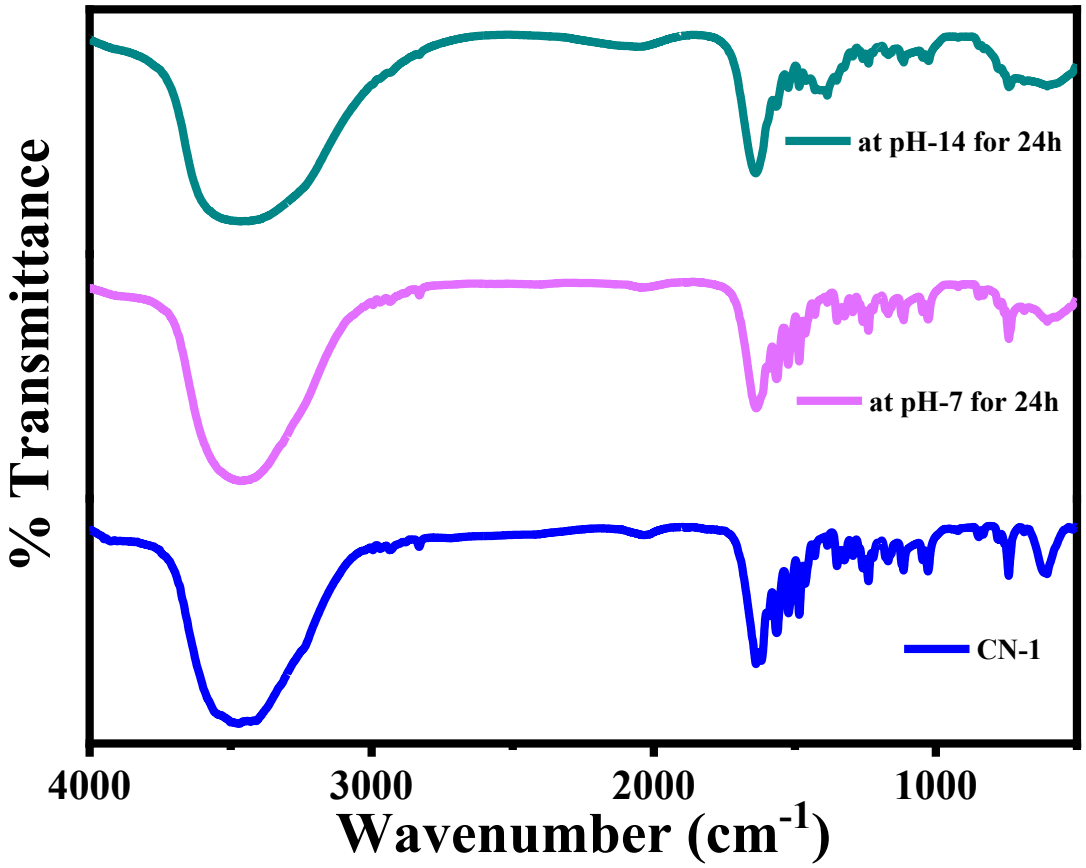

Fig. S5. FT-IR spectra for the pH stability of **CN-1.**

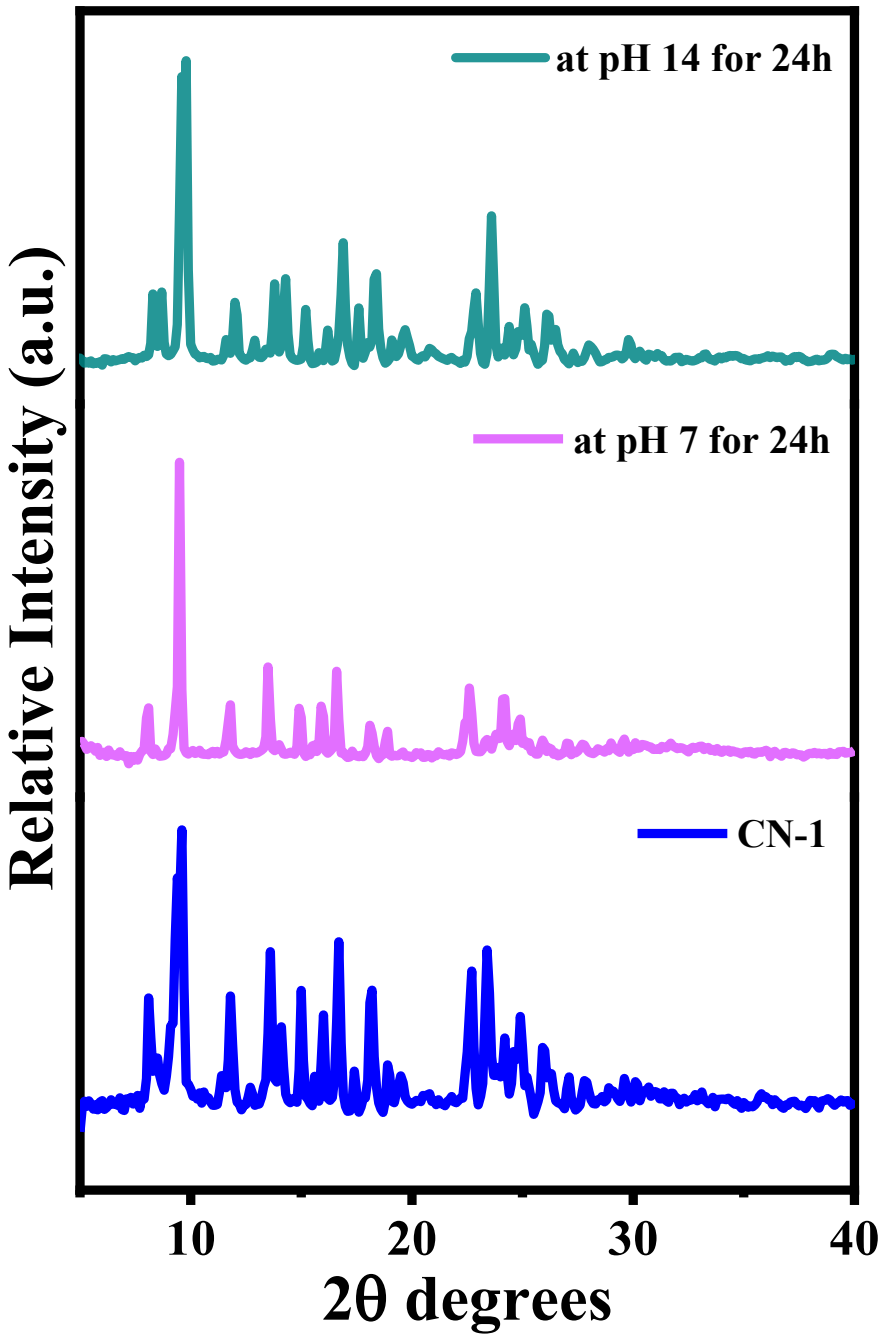

Fig. S6. PXRD pattern for the pH stability of **CN-1.**

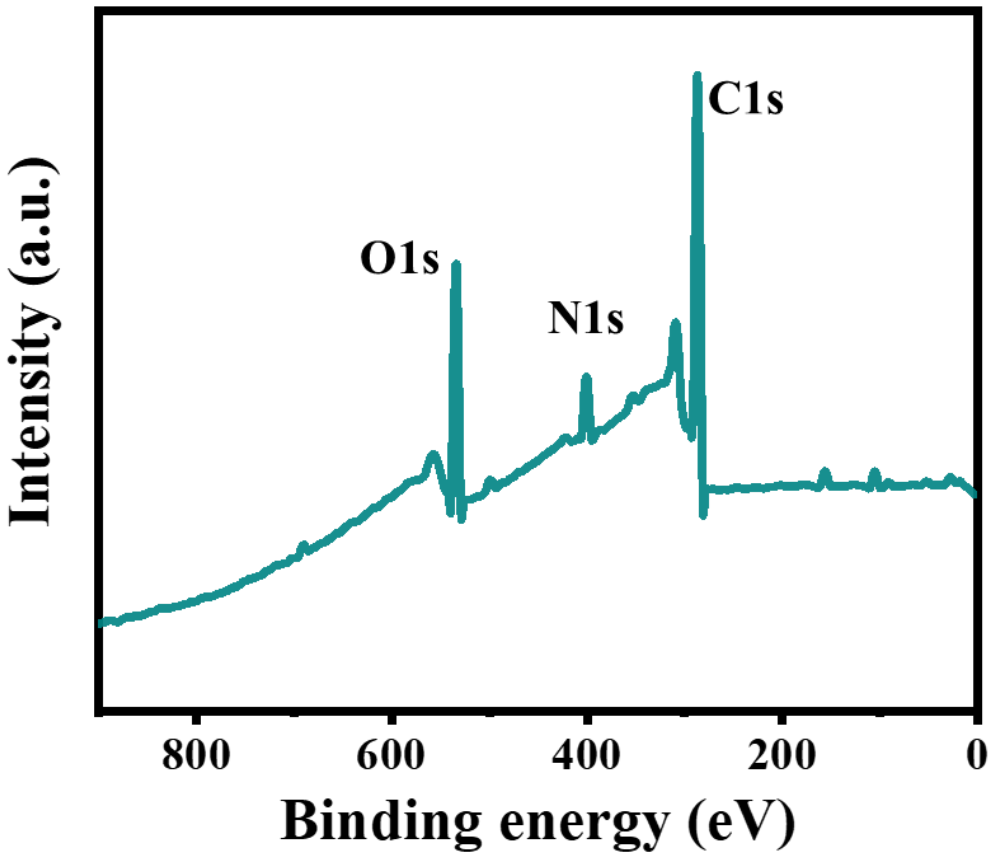

Fig. S7: XPS Survey Spectrum of **CN-1.**

Electrochemical Studies

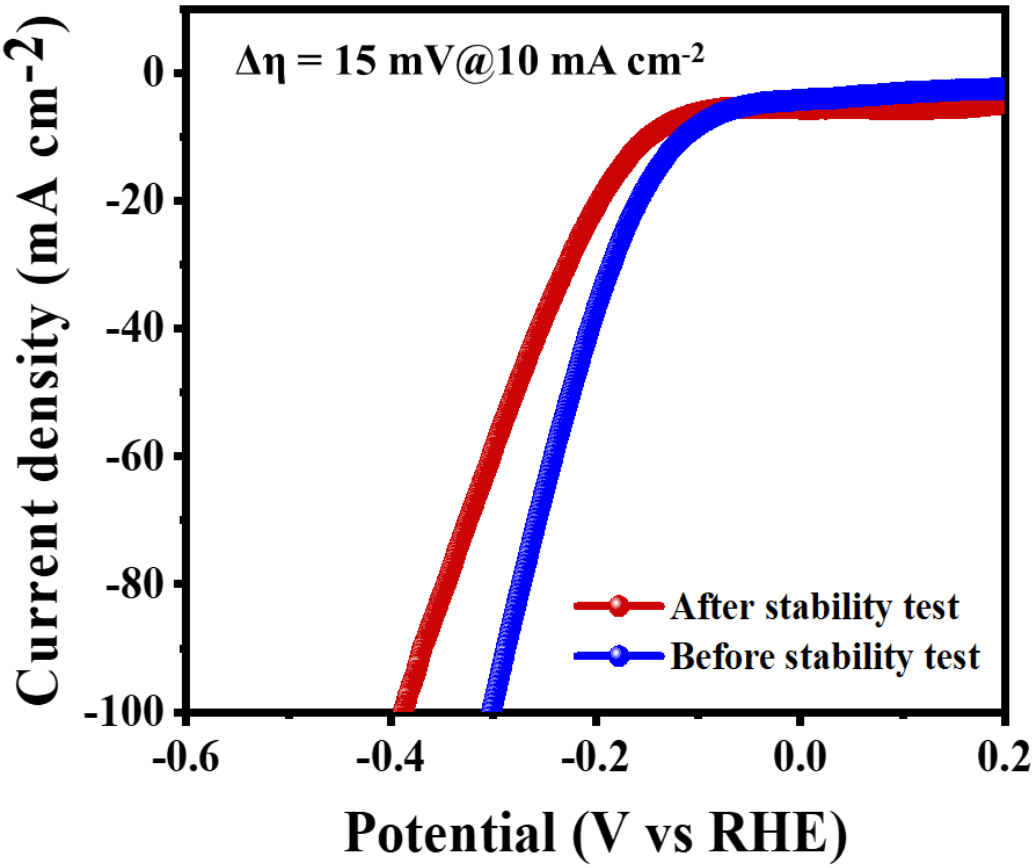

Fig. S8: LSV curve before and after catalysis of **CN-1**

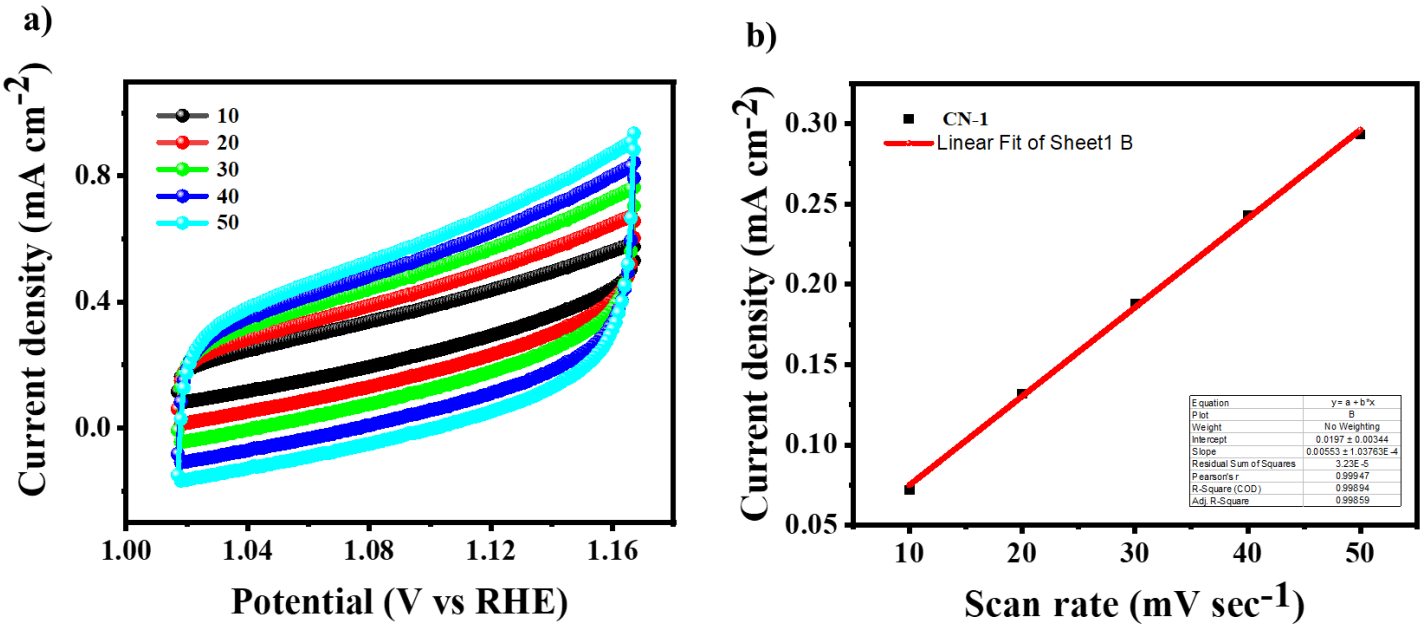

Fig. S9: Non-Faradaic CV and C_{dl} plot of **CN-1** at 1M KOH.

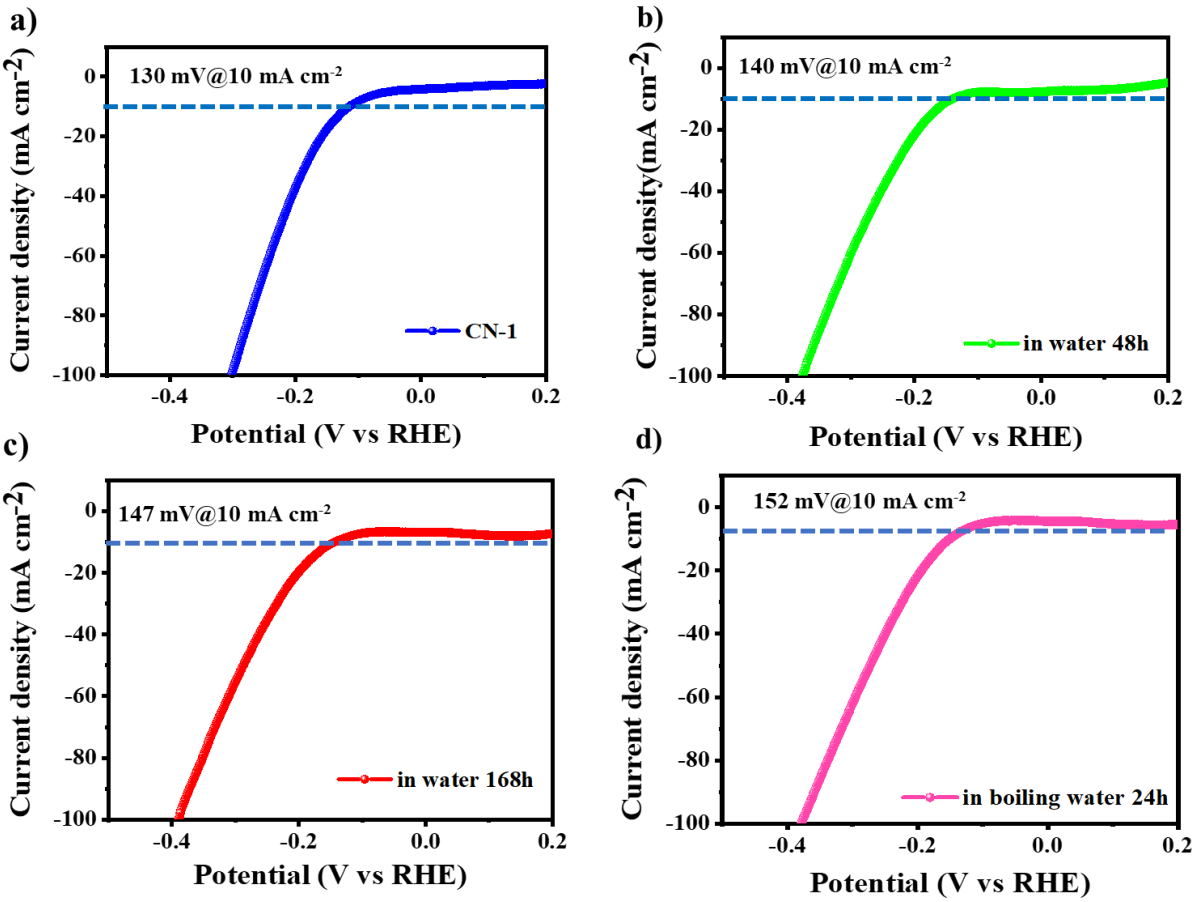

Fig. S10: Polarisation curve of **CN-1** at different hydrolytic conditions, a) 12 h, b) 48 h, c) 168 h, d) in boiling water 24 h.

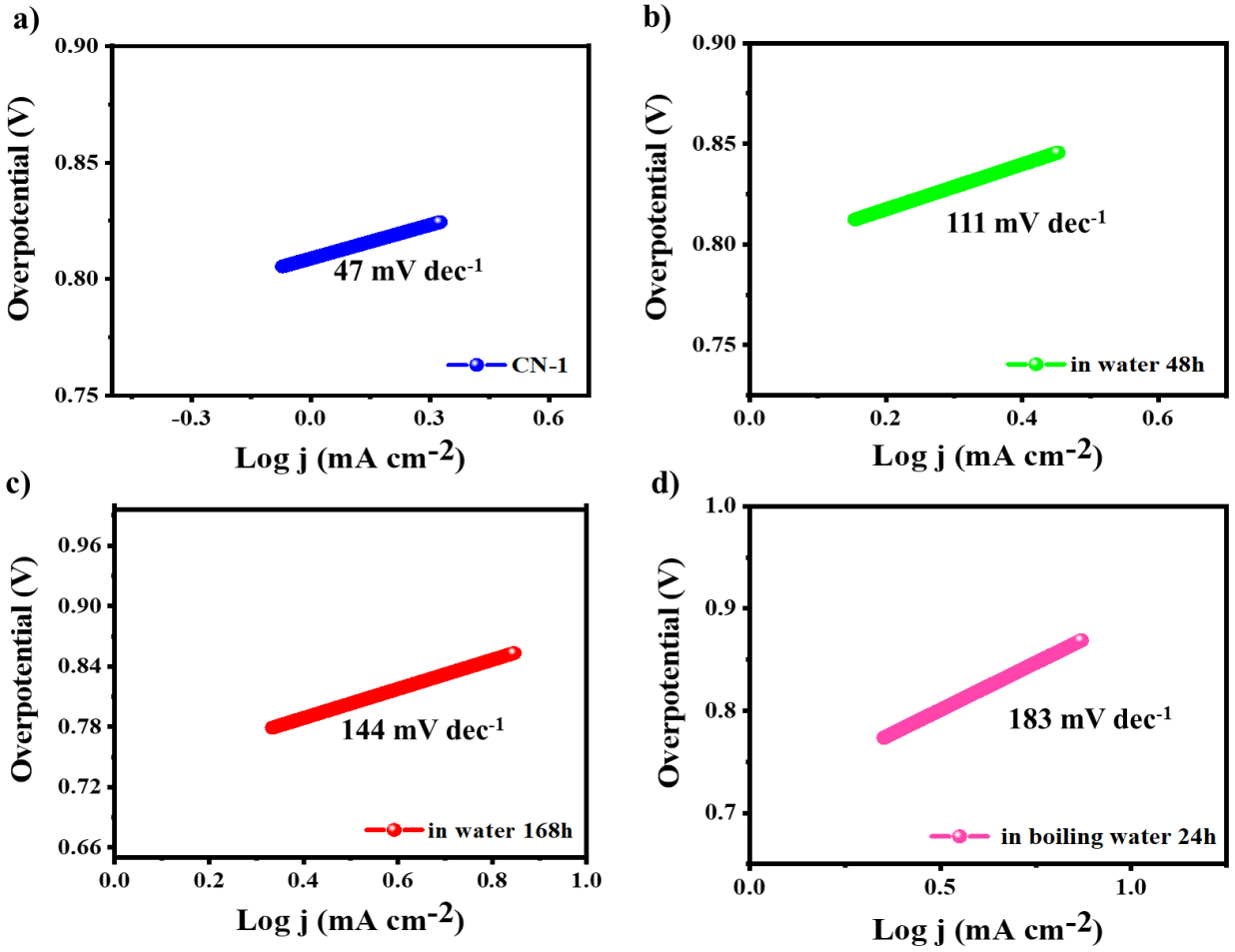

Fig. S11: Tafel slopes of **CN-1** at different hydrolytic conditions, a) 12 h, b) 48 h, c) 168 h, d) in boiling water 24 h.

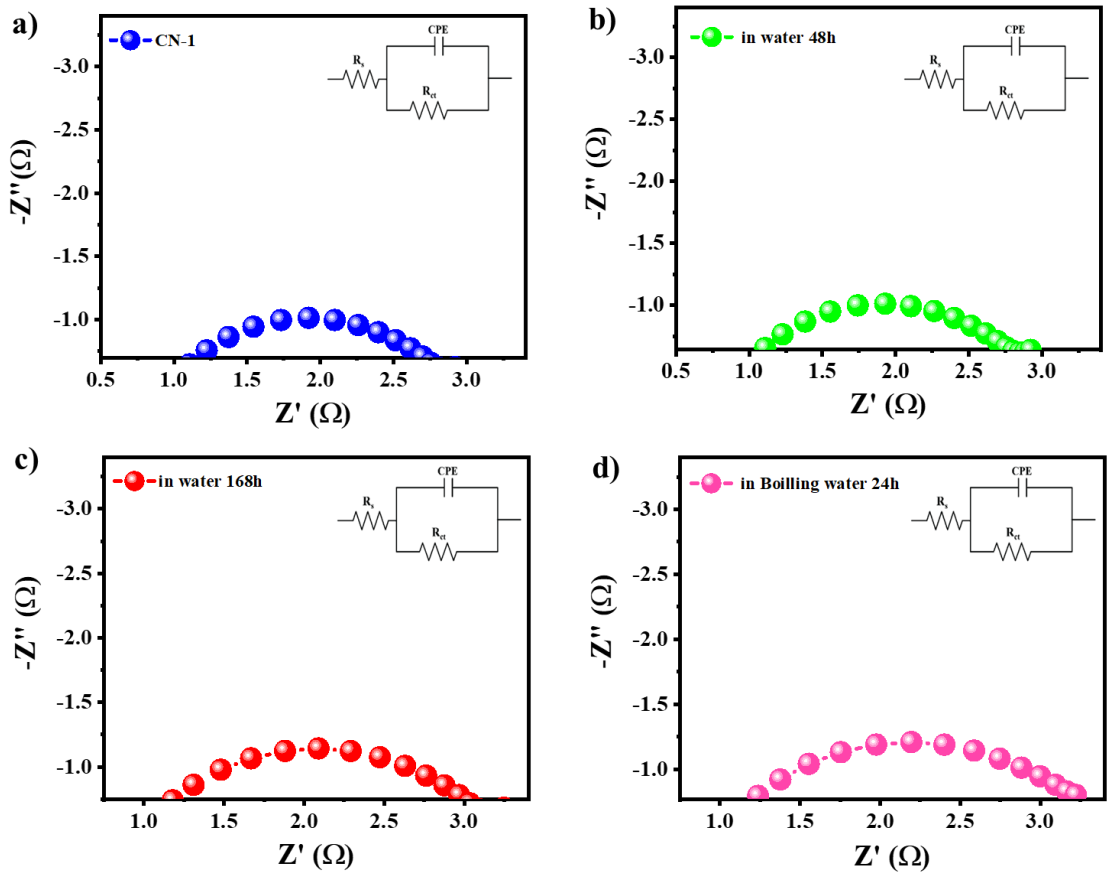

Fig. S12: Nyquist plots of **CN-1** at different hydrolytic conditions, a) 12 h, b) 48 h, c) 168 h, d) in boiling water 24 h.

Post catalysis

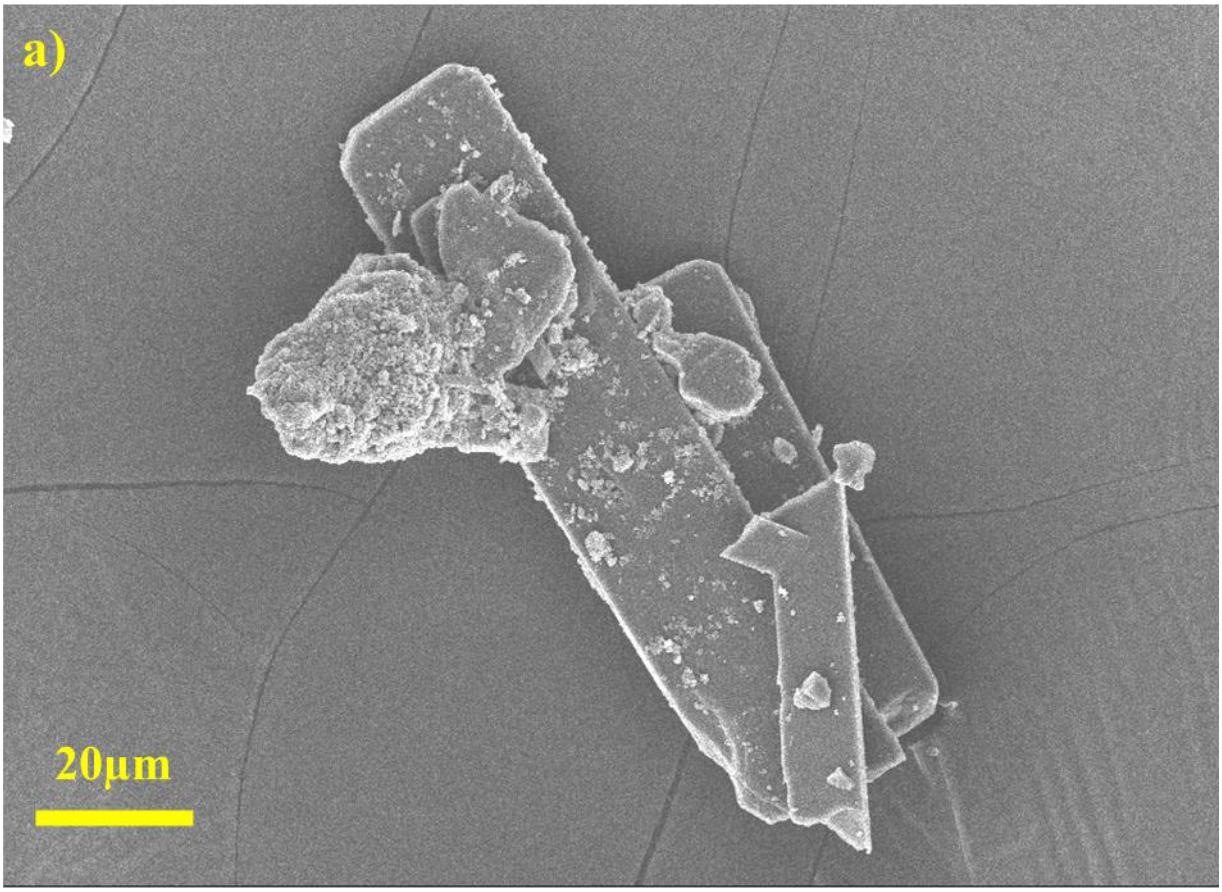

Fig. S13: SEM image after catalysis of **CN-1.**

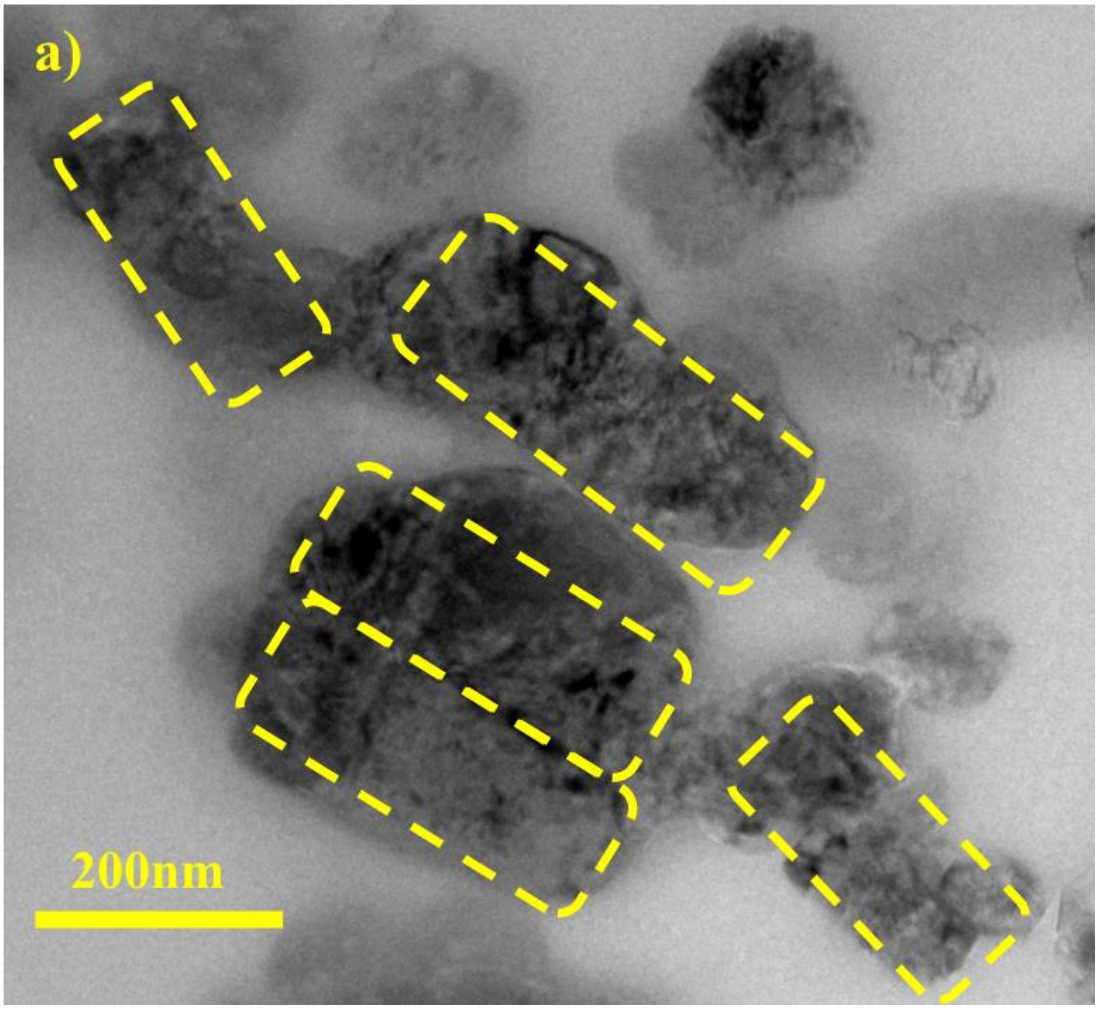

Fig. S14: TEM image after catalysis of **CN-1.**

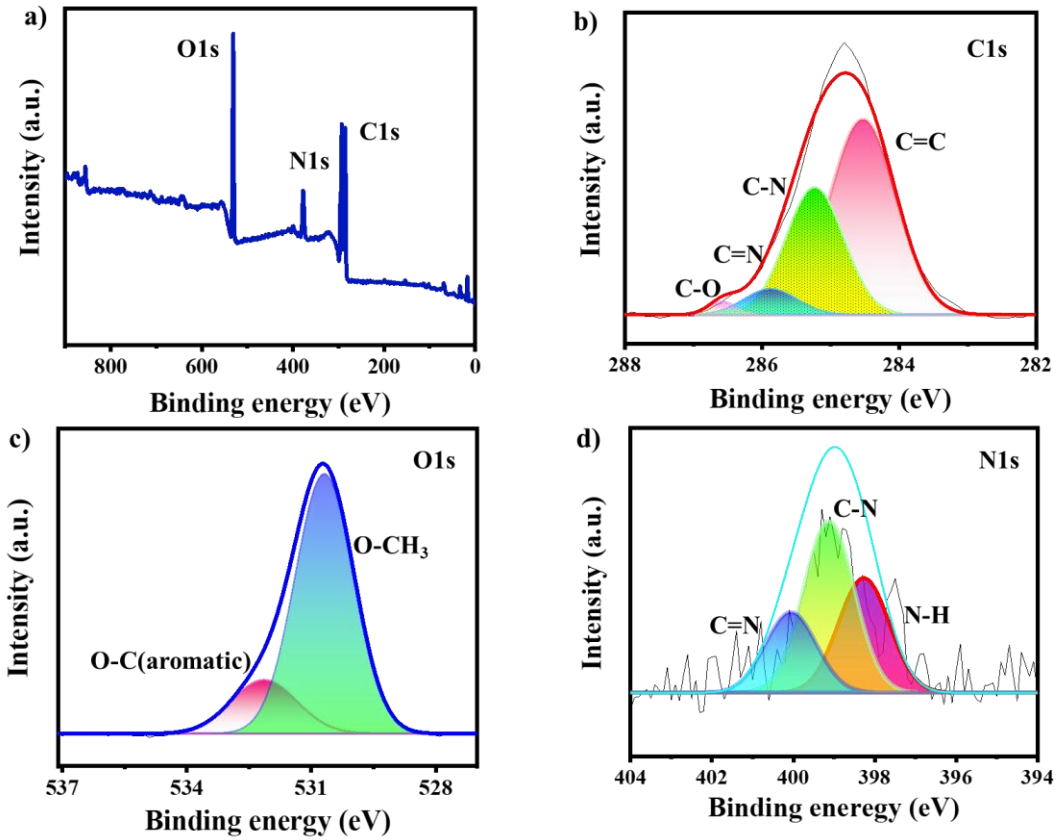

Fig. S15: XPS analysis after catalysis of **CN-1**

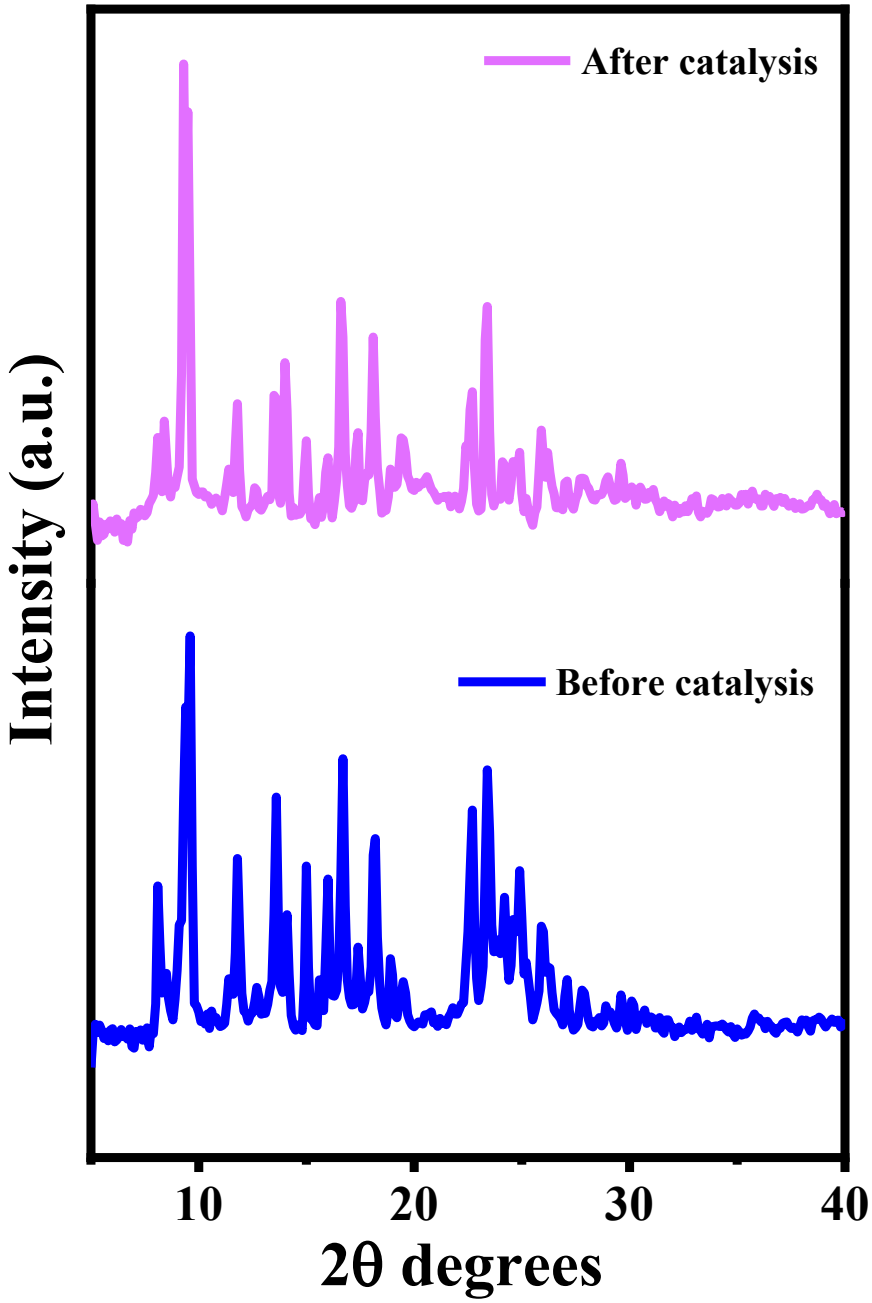

Fig. S16: PXRD analysis before and after catalysis of **CN-1**

Theoritical analysis

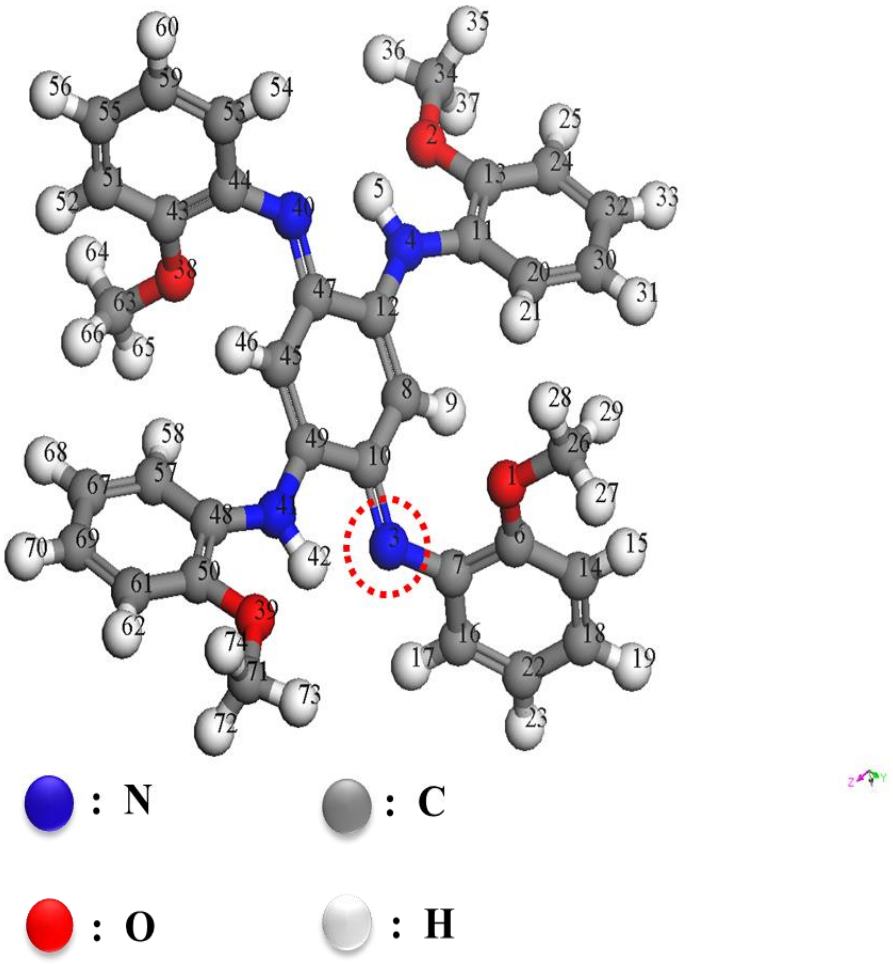

Fig. S17. Geometrically optimized structure for **CN-1**

Table S1: Analysis label and concentration average of iron regarding ICP-MS analysis.

Analysis label	**Concentration per run (57Fe)**		**Concentration average (57Fe)**
BLANK	1	0.000 ppm	0.000 ppm
0.05 ppm ME+Mix+Rb, Cs	1	0.042 ppm	0.042 ppm
	2	0.042 ppm	
	3	0.041 ppm	
0.1ppm ME+Mix+Rb, Cs	1	0.093 ppm	0.093 ppm
	2	0.095 ppm	
	3	0.092 ppm	
0.5 ppm ME+Mix+Rb, Cs	1	0.521 ppm	0.522 ppm
	2	0.520 ppm	
	3	0.523 ppm	
1.0ppm ME+Mix+Rb, Cs	1	0.986 ppm	0.990 ppm
	2	0.990 ppm	
	3	0.995 ppm	
CN 1	1	-0.009 ppm	**-0.009 ppm**
	2	-0.009 ppm	
	3	-0.009 ppm	

Table S2: Performance comparison of CN-1 at different hydrolytic conditions for the HER activity

Material	**HER (mV)**	**Tafel slope ($mV\ dec^{-1}$)**	**R_{ct} (Ω)**
CN-1	130	47	1.5
In water 48 h	140	111	1.6
In water 168 h	147	144	1.85
In boiling water 24 h	152	183	2

Table S3: Fukui (-) values for **CN-1**

Atoms	**Mulliken**	**Hirshfeld**
O1	0.009	0.012
O2	0.011	0.015
N3	**0.019**	**0.020**
N4	0.004	0.013
C6	0.010	0.012
C7	0.008	0.013
C8	0.009	0.014
C10	0.010	0.012
C11	0.013	0.013
C12	0.014	0.013
C13	0.015	0.015
C14	0.014	0.018
C16	**0.017**	**0.020**
C18	0.014	0.020
C20	0.012	0.016
C22	0.013	0.020
C24	0.014	0.019
C26	-0.004	0.010
C30	0.014	0.019
C32	0.014	0.020
C34	-0.003	0.011
O38	0.009	0.012
O39	0.011	0.015
N40	0.019	0.020
N41	0.004	0.013
C43	0.010	0.012
C44	0.008	0.013
C45	0.009	0.014
C47	0.010	0.012
C48	0.013	0.013
C49	0.014	0.013
C50	0.015	0.015
C51	0.014	0.018
C53	0.017	0.020
C55	0.014	0.020
C57	0.012	0.016
C59	0.013	0.020
C61	0.014	0.019
C63	-0.004	0.010
C67	0.014	0.019
C69	0.014	0.020
C71	-0.003	0.011

Table S4: Performance comparison of Metal free electrocatalysts for the HER activity

Sl No.	Material	Overpotential (mV at 10 mA cm^{-2})	Tafel Slope (mV dec^{-1})	Electrolyte	References
1.	D-AC	334 mV	66	0.5 M H_2SO_4	[2]
2.	SHG	310 mV	112	0.1 M KOH	[3]
3.	NCFs-800	114.3 mV	95.2	0.5 M H_2SO_4	[4]
4.	NCFs-800	198.6 mV	131.3	1 M KOH	
5.	N-VG	290 mV	121	0.5 M H_2SO_4	[5]
6.	TpPAM	250 mV	106	1 M KOH	[6]
7.	SHG	230 mV	112	1 M KOH	[3]
8.	Nr-HGM-1000	337 mV	99	0.5 M H_2SO_4	[7]
9.	Nr-HGM-1000	510 mV	157	0.1M KOH	
10.	GNP-900	179 mV	93	0.1 M KOH	[8]
11.	N,P–HCNF-8	550 mV	161	0.1 M KOH	[9]
12.	Ind-CPP	359 mV	64	0.5 M H_2SO_4	[10]
13.	Ind-CPP	364 mV	73	1 M KOH	
14.	GO-PANi31-FP	0.52 V		1 M KOH	[11]
15.	HT-AFNG	350 mV	113	0.5 M H_2SO_4	[12]
16.	AFNG	372 mV	120	0.5 M H_2SO_4	
17.	NG	564 mV	138	0.5 M H_2SO_4	
18.	**CN-1**	**130 mV**	**47**	**1 M KOH**	**This Work**

References

1 Y. Zheng, Y. Jiao, M. Jaroniec and S. Z. Qiao, *Angew. Chemie Int. Ed.*, 2015, **54**, 52–65.

2 X. Yan, Y. Jia, T. Odedairo, X. Zhao, Z. Jin, Z. Zhu and X. Yao, *Chem. Commun.*, 2016, **52**, 8156–8159.

3 C. Hu and L. Dai, *Adv. Mater.*, DOI:10.1002/adma.201604942.

4 J. Sun, Q. Ge, L. Guo and Z. Yang, *Int. J. Hydrogen Energy*, 2020, **45**, 4035–4042.

5 Y. Li, C. Ai, S. Deng, Y. Wang, X. Tong, X. Wang, X. Xia and J. Tu, *Mater. Res. Bull.*, 2021, **134**, 111094.

6 B. C. Patra, S. Khilari, R. N. Manna, S. Mondal, D. Pradhan, A. Pradhan and A. Bhaumik, *ACS Catal.*, 2017, **7**, 6120–6127.

7 J.-M. Ge, B. Zhang, L.-B. Lv, H.-H. Wang, T.-N. Ye, X. Wei, J. Su, K.-X. Wang, X.-H. Li and J.-S. Chen, *Nano Energy*, 2015, **15**, 567–575.

8 Z. Liu, M. Wang, X. Luo, S. Li, S. Li, Q. Zhou, W. Xu and R. Wu, *Appl. Surf. Sci.*, 2021, **544**, 148912.

9 Y. Gao, Z. Xiao, D. Kong, R. Iqbal, Q.-H. Yang and L. Zhi, *Nano Energy*, 2019, **64**, 103879.

10 I. Nath, J. Chakraborty, R. Lips, S. Dekyvere, J. Min, R. S. Varma and F. Verpoort, *J. Mater. Chem. A*, 2023, **11**, 10699–10709.

11 J. Zhang and L. Dai, *Angew. Chemie*, 2016, **128**, 13490–13494.

12 B. Deng, D. Wang, Z. Jiang, J. Zhang, S. Shi, Z.-J. Jiang and M. Liu, *Carbon N. Y.*, 2018, **138**, 169–178.